Transmission electron microscope studies of the crystal structure of $Y_2Cu_2O_5$ and the nature of nonperiodic planar defects in $Y_2Cu_2O_5$

1990 J. Phys.: Condens. Matter 2 5085

(http://iopscience.iop.org/0953-8984/2/23/001)

J. Phys.: Condens. Matter 2 (1990) 5085–5095. Printed in the UK

Transmission electron microscope studies of the crystal structure of $Y_2Cu_2O_5$ and the nature of non-periodic planar defects in $Y_2Cu_2O_5$

K Z Baba-Kishi†, R A Camps‡ and P A Thomas§

† Department of Physics, University of Essex, Colchester CO4 3SQ, UK

‡ Department of Metallurgy and Materials Science, University of Cambridge, Cambridge CB2 3QZ, UK

§ Clarendon Laboratory, University of Oxford, Parks Road, Oxford OX1 3TU, UK

Received 5 October 1989, in final form 28 February 1990

Abstract. An account is given of transmission electron microscope studies of the crystal structure of $Y_2Cu_2O_5$ discovered within samples of $YBa_2Cu_3O_{7-x}$ and $Y_{1.85}Sr_{0.15}CuO_{4-\delta}$ ceramic compounds. Conventional and high-resolution electron microscope investigations confirmed that $Y_2Cu_2O_5$ is isostructural with $Ho_2Cu_2O_5$ and has a space group $P2_1nb$ with lattice parameters $a = 1.247$ nm, $b = 1.081$ nm and $c = 0.3495$ nm. The nature of planar defects discovered within the crystallites of $Y_2Cu_2O_5$ is discussed. It is proposed that small amounts of barium that do not react to form a solid solution with $Y_2Cu_2O_5$ segregate to the lines of defects. The displacement vector for the planar defects was found to be $\frac{1}{2}[014]$.

1. Introduction

Since the discovery of high-T_c superconducting $YBa_2Cu_3O_{7-x}$ ceramics, the crystal structures of various compounds that are related to $YBa_2Cu_3O_{7-x}$ have attracted considerable attention. Among these, La_2CuO_4 is the most widely studied compound, for which two different space groups $Pccn$ or $Fmmm$ with lattice parameters $a = 0.533$ nm, $b = 0.5409$ nm and $c = 1.317$ nm have been proposed (Lorgo and Raccah 1973, Tanaka *et al* 1987). There are also the compounds of $(La_{1-x}Sr_x)_2CuO_{4-\delta}$, which undergo a superconducting phase transition at $\simeq$36 K, and have tetragonal symmetry with space group $I4/mmm$ and lattice parameters $a = b = 0.3777$ nm and $c = 1.3227$ nm (see, for example, Onoda *et al* 1987). It is also established that the $(La_{1-x}Sr_x)_2CuO_{4-\delta}$ phases are isostructural with those of $(Y_{1-x}Sr_x)_2CuO_{4-\delta}$. However, single-crystal x-ray diffraction studies have shown that the $(La_{1-x}Ba_x)_2Cu_{4-\delta}$ phases are orthorhombic, with possible space groups $Pccn$ or $Pccm$ and lattice parameters $a = 0.5378$ nm, $b = 0.5371$ nm and $c = 1.3234$ nm (Onodo *et al* 1987). It is believed that the space groups of the $(Y_{1-x}Ba_x)_2CuO_{4-\delta}$ phases are also identical with those of the $(La_{1-x}Ba_x)_2CuO_{4-\delta}$ crystals.

Recently, during an investigation of the microstructure of a ceramic sample of $YBa_2Cu_3O_{7-x}$, some isolated grains of $Y_2Cu_2O_5$ were discovered. It was also found that the microstructure of the grains of $Y_2Cu_2O_5$ was dominated by numerous planar defects. It was noted that the crystal structure of $Y_2Cu_2O_5$ has not been studied in detail, and

only some incomplete structural information was available in the literature. In addition, owing to similarities between the space groups and lattice parameters of various superconducting and non-superconducting compounds, identification of the crystal structure of the isolated grains of $Y_2Cu_2O_5$ at first proved difficult. The presence of planar defects within the grains made the identification process even more complex, because planar defects have also been observed to exist within some grains of La_2CuO_4 and $YBa_2Cu_3O_{7-x}$ (Davis and Tilley 1987, Zhou *et al*1987).

Conventional and high-resolution transmission electron microscopy methods have proved valuable in the characterisation of both the crystal structure of $Y_2Cu_2O_5$ and the nature of its planar defects. This paper describes the results of the TEM and x-ray diffraction studies of the structure of $Y_2Cu_2O_5$, and discusses some of the difficulties encountered in interpretation of the electron diffraction patterns obtained from the grains of $Y_2Cu_2O_5$. The study also aims to elucidate the nature of the planar defects in $Y_2Cu_2O_5$.

2. Experimental details

The ceramic samples used in the course of this study were produced by sintering powders that had mostly been prepared by the mixed oxide route. To prepare the samples of $YBa_2Cu_3O_{7-x}$, high-purity $BaCO_3$, CuO and Y_2O_3 powders were milled together for one hour in acetone. The ratio of Y^{3+}:Ba^{2+}:Cu^{2+}/Cu^{3+} in the mixture was 1:2:3. The resulting powder was calcined in air at 900–950 °C. The calcination product was then finely crushed and cold pressed at 80 MPa. The cold-pressed pellets were sintered in flowing oxygen at 900–950 °C and then cooled slowly to room temperature. The ceramic samples, which contained substantial amounts of $Y_2Cu_2O_5$ instead of the intended $Y_{1.85}Sr_{0.15}CuO_{4-\delta}$, were prepared by the spray-drying route. Specimens were prepared for study in the transmission electron microscope (TEM) by mechanical polishing, followed by argon-atom thinning. The microscopes used were a JEOL 200-CX and the purpose-built high-resolution electron microscope at the University of Cambridge.

3. Results and discussion

3.1. Analysis by electron diffraction

Figure 1(*a*) is a dark-field (DF) transmission electron micrograph illustrating the image of a heavily faulted grain discovered within a sample of $YBa_2Cu_3O_{7-x}$ high-T_c superconducting ceramic material. The image was obtained using a set of reflections indicated in the electron diffraction pattern shown in the inset of figure 1(*a*). It can be seen that the faults are crystallographically oriented. The electron diffraction pattern in the inset of figure 1(*a*) shows continuous streaking, and elongated reflections.The streaks are perpendicular to the fault planes, indicating that the streaks arise as a result of the faults within the grain.

Figure 1(*b*) is a DF low-magnification lattice image obtained using the reflections indicated in the inset of figure 1(*b*). It can be seen that the faults are planar, and they have one-dimensional disorder normal to the plane of the faults, which give rise to diffuse streaking in the electron diffraction patterns. Careful examination of the electron

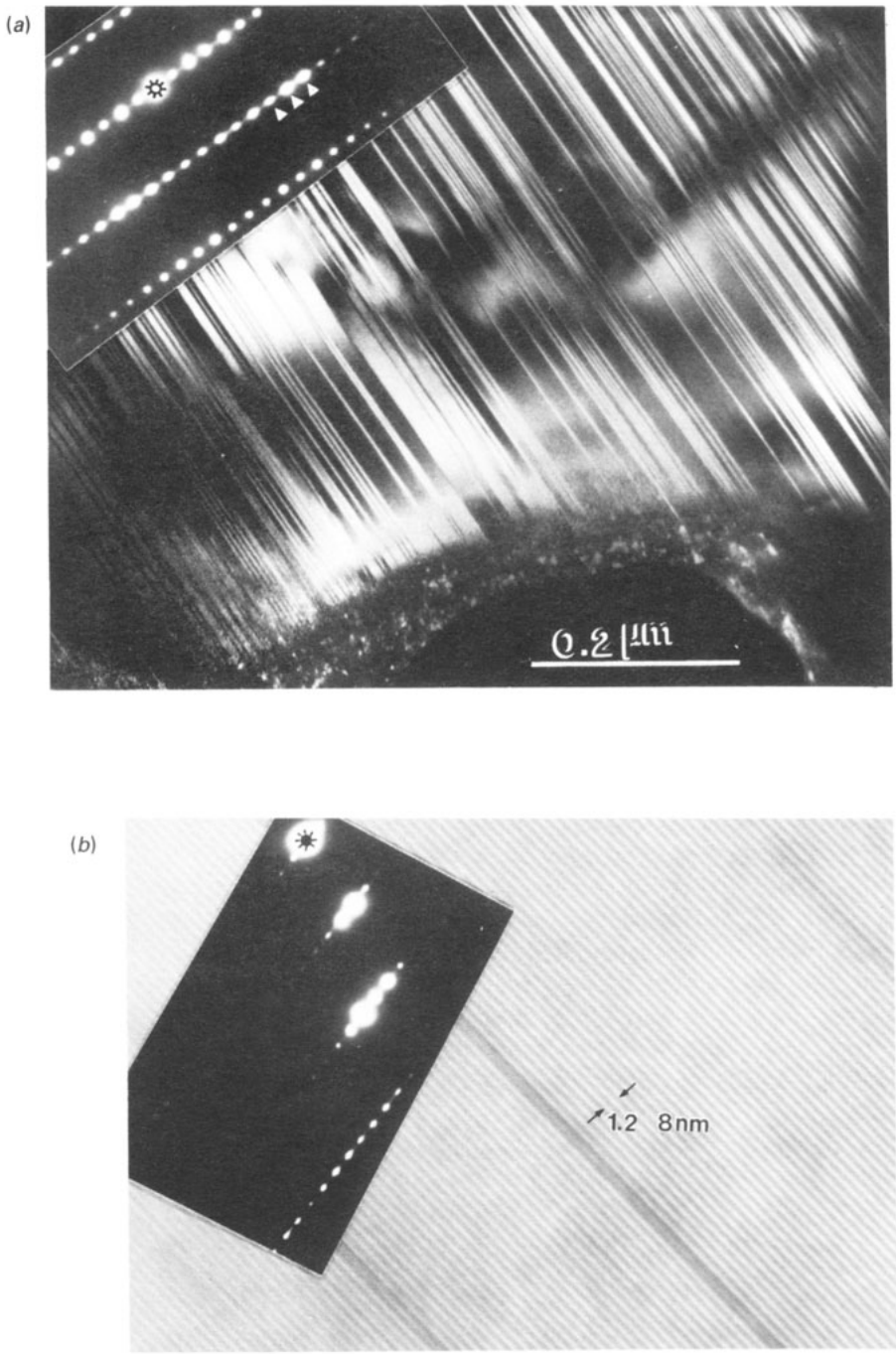

Figure 1. (*a*) A DF image showing a crystallite with numerous planar defects. The defect microstructure closely resembles the microstructure of the {110} twin domains in grains of $YBa_2Cu_3O_{7-x}$. The zone-axis electron diffraction pattern illustrates continuous streaking and elongated reflections. The image was obtained using a set of reflections indicated with arrows. (*b*) A low-magnification lattice image illustrating the planar character of the defects. Note that the direction of streaking is perpendicular to the defect planes.

diffraction patterns obtained from two different faulted grains revealed that the intensities of the streaks varied with the density of the faults.

The interplanar distances obtained from the diffraction pattern shown in the inset of figure 1(*a*) were compared with the interplanar distances of various compounds, including $(Y(La)_{1-x}Sr_x)_2CuO_{4-\delta}$ and $(Y(La)_{1-x}Ba_x)_2CuO_{4-\delta}$. It was found that the diffraction pattern could not be unambiguously indexed. However, similarities between the space group P_{ccn} of $(La(Y)_{1-x}(Ba)_x)_2CuO_{4-\delta}$ and that represented by the diffraction pattern of figure 1(*a*) were noted.

In order to understand better the structure of $Y_{2-x}Sr_xCuO_{4-\delta}$, a ceramic sample whose nominal composition was believed to be $Y_{1.85}Sr_{0.15}CuO_{4-\delta}$ was investigated by TEM. Extensive investigations revealed that the sample was substantially single phase and that all the grains were faulted. Surprisingly, the faults and the corresponding reflections showed marked similarities to those illustrated in figure 1(*a*). Electron diffraction patterns obtained from the faulted grains exhibited continuous streaking as exemplified in figure 2(*e*). DF electron micrographs obtained using streaked reflections showed heavily faulted microstructures. Examination of various faulted grains revealed that the concentration and number of planar faults varied considerably in each grain. Consequently, the intensities of the streaks varied with the density of the faults.

The crystals of $La_{2-x}(Ba)_xCuO_{4-\delta}$ and $La_{2-x}(Sr)_xCuO_{4-\delta}$ have the possible space groups P*ccn* or P*ccm* and I4/mmm respectively. It has also been established that replacing La with Y does not alter the space groups. Extensive study of the zone-axis electron diffraction patterns in figures 2(*a*)–(*f*), obtained from the faulted grains at various different orientations, showed that the patterns could not be unambiguously indexed according to P*ccn*, P*ccm* and I4/mmm. However, careful re-examination of the diffraction patterns shown in figures 2(*a*)–(*f*) revealed that the reflections can be unambiguously indexed according to the space group $P2_1nb$. This is the space group quoted for $Ho_2Cu_2O_5$, which has lattice parameters $a = 1.247$ nm, $b = 1.081$ nm and $c = 0.3495$ nm (Freund and Muller-Buschbaum 1977). The interplanar distances measured from the selected-area diffraction patterns in figures 2(*a*)–(*f*) showed close correspondence with the interplanar distances of $HO_2Cu_2O_5$. This observation indicated that the crystal structure of the ceramic material investigated could well be related to that of $Ho_2Cu_2O_5$. Hence, the space group $P2_1nb$, quoted for $Ho_2Cu_2O_5$, was used to index the selected-area diffraction patterns. It was found that the patterns could be unambiguously indexed according to $P2_1nb$. Therefore, it was concluded that the specimen was $Y_2Cu_2O_5$ with space group $P2_1nb$ (from isomorphism with the $Ho_2Cu_2O_5$ structure). It should be pointed out that the space group $P2_1nb$ could not have been deduced from the selected-area diffraction patterns alone, without a knowledge of the lattice parameters and the space group of $HO_2Cu_2O_5$. Hence, it can be deduced from the indexed selected-area diffraction patterns that the conditions for visibility of reflections are *hkl* for all orders, 0*kl* for all orders, *h*0*l* with $h + l = 2n$, *hk*0 with $k = 2n$, *h*00 with $h = 2n$ and 00*l* with $l = 2n$. Hence the crystal structure is primitive and the space group is $P2_1nb$. In order to confirm the results of the TEM investigations, some preliminary x-ray powder diffraction studies of the ceramic samples were carried out. The findings of the x-ray diffraction studies are described in § 3.2.

To index the patterns according to $P2_1nb$, it was also assumed that the 100 reflection, present in all the diffraction patterns along the systematic row of reflections, marked $\boldsymbol{a}^*$, is not permitted and arises as a result of double diffraction. Numerous tilting experiments revealed that the intensity of the 100 reflection varied significantly with both the orientation of the sample, with respect to the electron beam, and the thickness of the sample.

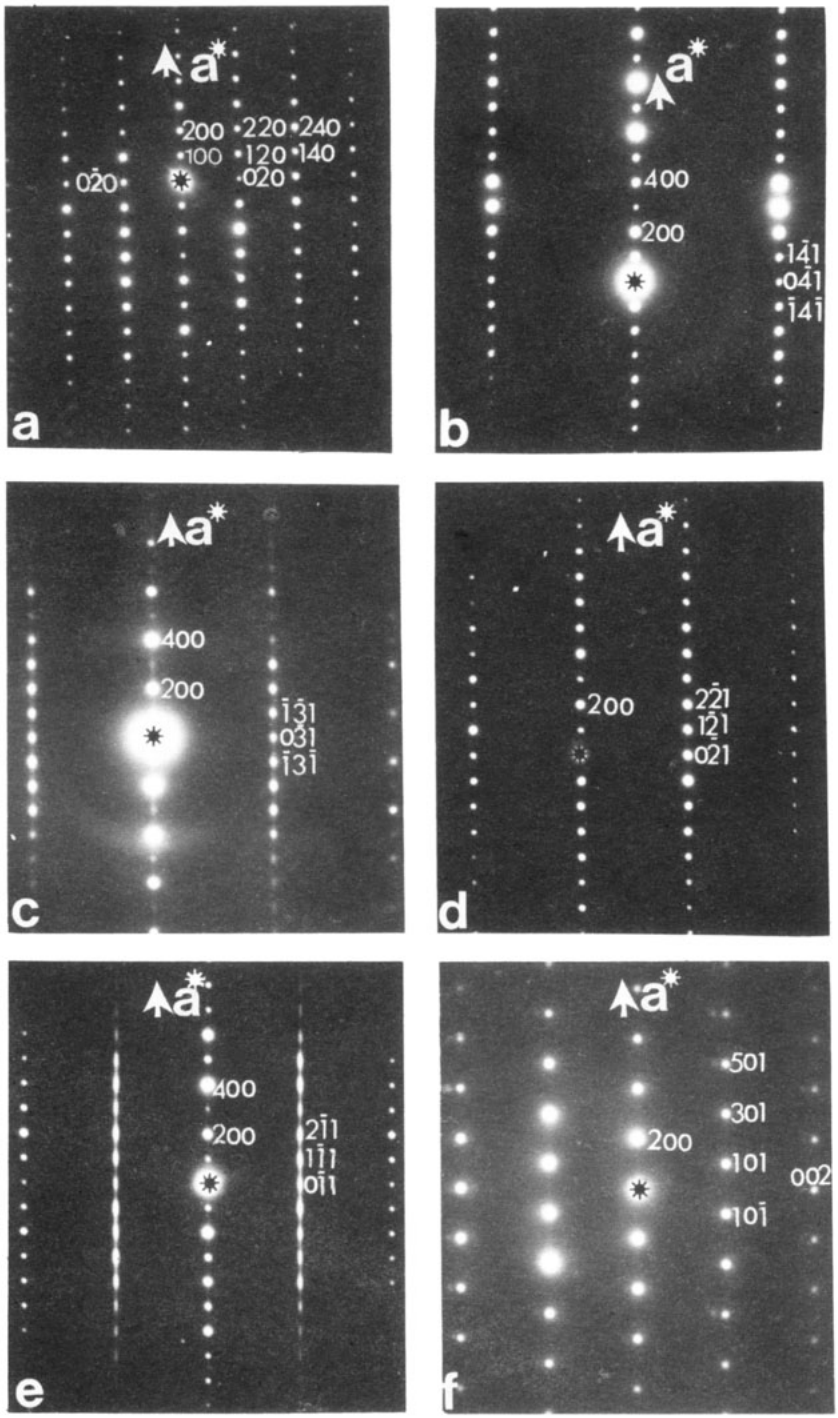

Figure 2. Zone-axis electron diffraction patterns obtained from crystallites of $Y_2Cu_2O_5$. The patterns (*d*)–(*f*) correspond to the zone axes [001], [014], [013], [012], [011] and [010] respectively. The patterns were unambiguously indexed using the space group $P2_1nb$, and lattice parameters $a = 1.248$ nm, $b = 1.081$ nm and $c = 0.3495$ nm. Note that the streaks can only be observed in the diffraction patterns corresponding to the zone axes [011] and [013]. Also note that the 100 forbidden reflection arising from double diffraction is not present in (*f*), which was taken with the electron beam almost parallel to the [010] zone axis.

This evidence is consistent with the presence of a reflection that arises as a result of double diffraction. The presence of a reflection arising from double diffraction can also be determined by adding a pair of appropriate reciprocal lattice vectors. For example, if the reciprocal lattice vectors, represented by the reflections 120 and $0\bar{2}0$ in figure 2(*a*), are added, then the forbidden 100 reflection can be generated. It is therefore proposed that both the phases observed within the samples of $YBa_2Cu_3O_{7-x}$ and $Y_{1.85}S_{0.15}CuO_{4-\delta}$ are $Y_2Cu_2O_5$, which contains little or no barium or strontium. Furthermore, it is proposed that strontium and barium do not react to form a solid solution with the matrix of $Y_2Cu_2O_5$, and consequently they concentrate at the lines of the defects observed within the grains.

The electron diffraction patterns shown in figures 2(*a*)–(*f*) correspond to the zone axes [001], [014], [013], [012], [011] and [010] respectively. Tilting the specimen away from [001], along the reciprocal lattice vector $\boldsymbol{a}^*$, showed that the streaks were confined to the [013] and [011] zone axes (figures 2(*c*) and (*e*)). The strong streaking is observed in each case to lie parallel to alternate systematic rows. DF images obtained with the streaked reflections revealed that the faults are planar in nature, and do not possess long-range periodicity.

It is possible to determine the displacement vector associated with the planar faults, using the relationship

$$\boldsymbol{R} \cdot \boldsymbol{g}_i = n_i \qquad i = 1, 2, 3$$

where $n_i = [\alpha, \beta, \gamma]$ is zero or an integer, $\boldsymbol{g}_i$ is the reciprocal lattice vector, and $\boldsymbol{R} = [uvw]$ is the displacement vector. In order to determine the displacement vector, it is necessary to find three linearly independent reciprocal lattice reflections, $\boldsymbol{g}_i$, for which the planar defects are invisible (Van Der Biest and Thomas 1976). It is also necessary to keep the integers, n_i arbitrary, which is achieved by selecting the lowest-order reflections along a systematic row. Careful and extensive tilting of the specimen along various systematic rows of reflections, and subsequent imaging under two-beam conditions, established that the planar faults became invisible using various reflections, including 220, $0\bar{4}1$ and $1\bar{2}1$. As expected, the planar faults became visible using the reflections $0\bar{3}1$, $\bar{1}3\bar{1}$, $0\bar{1}1$ and $1\bar{1}1$ which are indicated in the diffraction patterns of figure 2(*c*) and (*e*). Hence, substituting the reflections for which the faults were out of contrast into the equation $\boldsymbol{R}_i \cdot \boldsymbol{g}_i = n_i$, we can obtain

$$+2u + 2v = \alpha \qquad -4v + w = \beta \qquad +u - 2v + w = \gamma.$$

Hence, the displacement vector $\boldsymbol{R}$ is given by

$$\boldsymbol{R} = [\alpha + \beta - \gamma, (-\alpha - 2\beta + 2\gamma)/2, -2\alpha - 3\beta + 2\gamma].$$

For $\alpha = 1$, $\beta = 0$ and $\gamma = 1$, the displacement vector is $\boldsymbol{R} = \frac{1}{2}[014]$. This indicates that the displacement vector has no component along the x direction, which can be confirmed by the lack of streaking along the systematic rows, marked $\boldsymbol{a}^*$ in figures 2(*a*)–(*f*).

It is reasonable to assume that the planar faults may well be sequence faults, which are non-conservative in nature, since their existence necessarily requires a change in chemical composition. This change in composition arises from unreacted $SrCO_3$ and $BaCO_3$ which segregate, thus forming the slabs of defects that have chemical compositions different to that of $Y_2Cu_2O_5$.

To get a better understanding of the crystal structure of $Y_2Cu_2O_5$, and the nature of planar defects, some high-resolution electron microscope (HREM) studies were carried out. Figures 3(*a*), (*b*) and (*d*) present the high-resolution lattice images of $Y_2Cu_2O_5$ obtained with the electron beam parallel to the [001] direction. The lattice images were

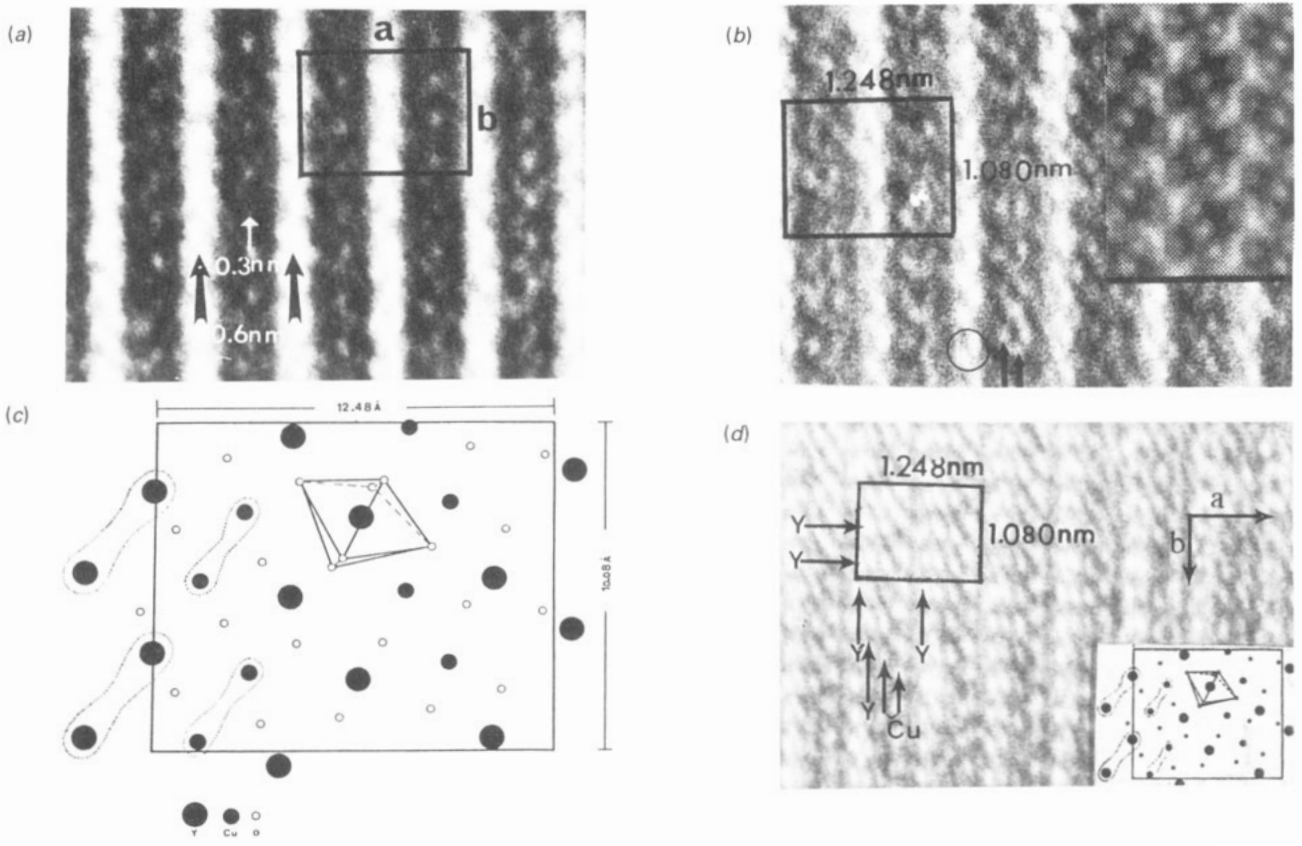

Figure 3. (*a*) A high-resolution electron micrograph of a $Y_2Cu_2O_5$ crystal, obtained with the electron beam parallel to the [001] zone axis, at a microscope defocus $\simeq -64$ nm. A unit cell with $a = 1.248$ nm and $b = 1.080$ nm is indicated. (*b*) A high-resolution lattice image of a $Y_2Cu_2O_5$ crystal, obtained at a defocus value of $\simeq +32$ nm, with the beam parallel to [001]. The unit cell is outlined. A pair of yttrium atoms is circles. Copper atoms are arrowed. The inset in (*b*) shows a calculated [001] image at $\Delta f = 50$ nm for the crystal that is 3.5 nm thick. (*c*) A structure model of $Y_2Cu_2O_5$ projected along [001]. Large full circles indicate the projection of yttrium sites. Pairs of yttrium atoms were frequently seen as 'dumb-bell' shapes in the lattice images. The projection corresponds to the unit cell indicated in the lattice images. (*d*) A high-resolution lattice image of a $Y_2Cu_2O_5$ crystal, obtained at a defocus $\simeq -128$ nm. A unit cell is outlined. The inset is a projected [001] structure of $Y_2Cu_2O_5$, and corresponds to the unit cell outlined in the lattice image.

produced without using an objective aperture, and all the reflections present in the [001] electron diffraction pattern, illustrated in figure 2(*a*), could potentially contribute to the images. The images were obtained using the 500 keV TEM, which has a nominal resolution of ≈0.2 nm.

Figure 3(*a*) reveals an approximately square arrangement of bright spots. The separation of the thick fringes, indicated with solid arrows, is approximately 0.6 nm, and corresponds to the *d*-spacings of the $\bar{2}00$ crystal planes. The less intense fringes have a separation of approximately 0.3 nm, and hence represent the *d*-spacing of the $\bar{4}00$ planes. Since the unit cell has a *b*-glide parallel to the [001] direction, the low-index reflections permitted are $\bar{2}00$ and $0\bar{2}0$. Thus, the unit cell has a periodicity of 1.248 nm along the lattice vector ***a*** and 1.080 nm along the lattice vector ***b*** as indicated in figure 3(*b*).

The structure model of $Y_2Cu_2O_5$ projected on a (100) lattice plane along the [001] direction is shown in figure 3(*c*). The structure model is identical to that of $Ho_2Cu_2O_5$, as described by Freund and Muller-Buschbaum (1977), and consists of four rows of yttrium and four rows of copper atoms along the *b* direction within the unit cell. Each atom of yttrium is located at the centre of an oxygen-sharing octahedron. A comparison of the lattice image in figure 3(*b*) with both the structure model and the computed image shown in the inset of figure 3(*b*) reveals that the $\bar{2}00$ and $\bar{4}00$ planes are coincident with the layers of yttrium and copper atoms respectively. Although the lattice image shown in figure 3(*b*) appears to be in good agreement with the structure model of $Y_2Cu_2O_5$, the distributions of intensities associated with the rows of yttrium atoms and those of copper atoms are complex. There are the regions where the rows of fringes corresponding to the atoms of yttrium exhibit 'dumb-bell' shapes, indicating that the individual columns of yttrium atoms, as described in the structure model, have not been resolved satisfactorily. Similarly, the copper atoms are seen as faint 'dumb-bells' in the lattice images.

It should be pointed out that direct interpretation of the lattice images was not readily possible. However, comparison of the images with the known structure model of $Ho_2Cu_2O_5$ and the computed images allowed an indirect interpretation of the lattice images to be achieved. The details of the computed images were strongly dependent on the specimen thickness and defocus conditions, and in the absence of any reliable data about the actual specimen thickness, numerous computed images had to be created. The computed image, shown in the inset of figure 3(*b*), is seen to agree closely with the experimentally obtained lattice images.

As expected, the information contained within the lattice images was strongly dependent on both the specimen thickness and the amount of microscope defocus. The image shown in figure 3(*d*) was obtained from a thin region very close to the edge of a grain, at a defocus of ≈128 nm. Although the details of the image vary with small changes in the specimen thickness, the information contained in the image corresponds closely to the structure model shown in the inset of figure 3(*d*). Unlike in the lattice image in figure 3(*b*), individual columns of yttrium and copper atoms are just visible in the pattern.

3.2. Analysis by x-ray powder diffraction

X-ray powder diffraction was used to support the findings of the TEM studies. Data were collected in the flat-plate transmission mode using a Stoe Stadi-2P diffractometer employing Cu Kα radiation. The resulting powder pattern showed strong similarities to the published x-ray powder diffraction data (*JCPDS* No 33-511 1981) for $Y_2Cu_2O_5$. However, several small additional peaks appeared and the intensity ratios were slightly different. On examination of the powder pattern, the extra peaks were found to cor-

respond to those expected for Y_2O_3, which was in the starting composition for the ceramic. The presence of Y_2O_3 also accounted for changes in the intensity ratios because there was some overlap of the peaks for the two phases.

$Y_2Cu_2O_5$ was reported in *JCPDS* to be orthorhombic with space group $Pna2_1$ and lattice parameters $a = 1.0799$ nm, $b = 0.3490$ nm and $c = 1.2456$ nm. When the Y_2O_3 peaks were excluded, the remaining 15 peaks were used for indexing the main $Y_2Cu_2O_5$ phase. The indexing procedure gave a primitive orthorhombic cell with refined lattice parameters of $a = 1.0791(6)$ nm, $b = 0.3497(2)$ nm and $c = 1.2473(6)$ nm. The refined d-spacings, 2θ-values and *hkl*s are given in table 1. The unit cell volume found for our

Table 1. Refined d-spacings, 2θ-values and *hkl*s for $Y_2Cu_2O_5$.

$Pna2_1$	$P2_1nb$	d (nm)	2θ (deg)	$Pna2_1$	$P2_1nb$	d (nm)	2θ (deg)
202	220	0.4081	10.87	205	520	0.2262	19.90
110	011	0.3334	13.35	006	600	0.2078	21.75
203	320	0.3292	13.50	412	241	0.2021	22.40
210	021	0.2935	15.21	413	341	0.1900	23.92
211	121	0.2857	15.63	414	441	0.1762	25.92
204	420	0.2699	16.58	020	002	0.1747	26.15
013	301	0.2675	16.73	610	061		
212	221	0.2652	16.88				

sample is sightly larger than that reported previously. This observation may be explained by the incorporation of a small amount of Sr^{2+} into the structure on the Y^{3+} site, as the former has a larger ionic radius. It was not possible to analyse the Sr^{2+} content of the compound from the two-phase powder data. However, the change in lattice parameters was sufficiently small to suggest that the compound corresponded very closely to stoichiometric $Y_2Cu_2O_5$.

It should be added that space group $Pna2_1$ implies that the 2_1 screw axis is parallel to c, the a-glide is in the (010) plane and the n-glide is in the (100) plane. This is identical with the unit cell quoted for $Ho_2Cu_2O_5$, which has lattice parameters $a = 1.247$ nm, $b = 1.081$ nm and $c = 0.3495$ nm, (Freund and Muller-Buschbaum 1977). The space group of $Ho_2Cu_2O_5$ is $P2_1nb$ (C_{2v}^9, No 33), indicating that the 2_1 screw axis is parallel to a, the b-glide is in the (001) plane and the n-glide is in the (010) plane. It follows, therefore, that if the $P2_1nb$ unit cell description is used, the *hkl*s listed in table 1 must be permutated. The transformation matrix taking the indices of *hkl* from $Pna2_1$ (old) to $P2_1nb$ (new) is

$$\begin{pmatrix} h_{\text{new}} \\ k_{\text{new}} \\ l_{\text{new}} \end{pmatrix} = \begin{pmatrix} 0\,0\,1 \\ 1\,0\,0 \\ 0\,1\,0 \end{pmatrix} \begin{pmatrix} h_{\text{old}} \\ k_{\text{old}} \\ l_{\text{old}} \end{pmatrix}.$$

4. Concluding remarks

In this study, we have discussed two different problems: (i) the crystal structure of $Y_2Cu_2O_5$; and (ii) the nature and possible causes of extensive planar defects found within the grains of $Y_2Cu_2O_5$. The crystal structure of $Y_2Cu_2O_5$, investigated using both the electron and x-ray diffraction techniques, is consistent with the crystal structure of

$Ho_2Cu_2O_5$, which has a space group $P2_1nb$. Electron diffraction patterns from $Y_2Cu_2O_5$, obtained with the electron beam parallel to various zone axes, including 001, 014, 012, 011, 013 and 010, were unambiguously indexed according to $P2_1nb$, with lattice parameters $a = 1.248$ nm, $b = 1.080$ nm and $c = 0.3495$ nm. Although extra forbidden reflections were observed along the $h00$ systematic rows, their existence was attributed to double-diffraction effects.

High-resolution electron microscope investigations further confirmed that the crystals of $Y_2Cu_2O_5$ are isostructural with those of $Ho_2Cu_2O_5$. Direct interpretation of lattice images was not always possible because fine details in them varied significantly with crystal thickness and microscope defocus. However, it was possible to identify individual columns of yttrium and copper atoms in some of the lattice images. In general, the projected atomic structures provided by the lattice images were in good agreement with both the computed images and the known crystal structure model of $Ho_2Cu_2O_5$. As expected, evidence for the presence of oxygen atoms was not observed in the lattice images.

Electron diffraction studies enabled some of the characteristics of the faults to be understood. The faults were observed to be planar, existed in variable numbers and were distributed randomly parallel to the (200) crystal planes. The exact nature of the defect chemistry and the crystal structure of the faults could not be determined, but the presence of streaking in the electron diffraction patterns indicated that the faults constitute chemical and structural characteristics different to those of $Y_2Cu_2O_5$. The faults were always observed when the electron beam was allowed to encompass the crystals along the [011] and [013] directions. The reasons for this phenomenon are not understood.

HREM investigations confirmed that complete rearrangement of atoms within the lines of faults had occurred. Although it proved difficult to establish a definite model as to the nature of the structure of the faults, it is thought highly probably that strontium or barium that had failed to react to form a solid solution segregated to the faults. It is envisaged that the concentration of strontium or barium within yttrium-deficient regions of the crystal would result in crystallographic shearing, thus allowing one slab of the crystal to be displaced relative to another slab. It is also anticipated that non-periodic distribution of barium or strontium atoms within the lines of faults will take place. In addition, the role of oxygen non-stoichiometry in the formation or perhaps retaining of the planar faults was not apparent. It seems reasonable to assume, however, that the formation of $Y_2Cu_2O_5$ instead of $YBa_2Cu_3O_{7-x}$ resulted in the structure of $Y_2Cu_2O_5$ collapsing along the (200) planes, thus generating random arrays of faults by accommodating unreacted barium. It is also thought that the fundamental processes that led to the formation of $Y_2Cu_2O_5$, and subsequent creation of planar faults, may well have been initiated by a disturbance in oxygen stoichiometry.

Acknowledgments

We thank the Allen Clark Research Centre, Caswell, and staff at Oxford University for the provision of ceramic samples. Our thanks are also due to Professor David Barber for useful discussions.

References

Davis A H and Tilley R J D 1987 *Nature* **326** 859–61

Freund H R and Muller-Buschbaum H K 1977 *Z. Naturf.* **326** 609–11
JCPDS No 33-511 1981 *Mineralogisch-Petrographisches, University of Heidelberg, Grant-in-Aid Report*
Lorgo L M and Raccah P M 1973 *J. Solid State Chem.* **6** 526–31
Onoda M, Shamato S, Sato M and Hosoya S 1987 *Japan. J. Appl. Phys.* **26** L363–5
Tanaka M, Tsudaz K, Yamada K, Endoh Y, Hidaka Y, Oda M, Suzuki M and Murakami T 1987 *Japan. J. Appl. Phys.* **26** L1502–4
Van Der Biest O and Thomas G 1976 *Electron Microscopy in Mineralogy* ed H R Wenk (Berlin: Springer)
Zhou W, Thomas J M, Jefferson D A, Mackay K D, Shen T H, Van Damme I and Liang W Y 1987 *J. Phys. F: Met. Phys.* **17** L173–6